Proceedings of ECOS 2009
Copyright © 2009 by ABCM

22nd International Conference on Efficiency, Cost, Optimization
Simulation and Environmental Impact of Energy Systems
August 31 – September 3, 2009, Foz do Iguaçu, Paraná, Brazil

DESIGN OF A COMBUSTION CHAMBER TO BURN LEATHER RESIDUALS GASIFICATION GAS

Cristiano Vitorino da Silva, cristiano@uricer.edu.br
Arthur Bortolin Beskow, arthur@uricer.edu.br
Department of Engineering and Computational Science, Universidade Regional Integrada do Alto Uruguai e das Missões - URI.
GEAPI – Group of Applied Engineering to Industrial Processes.
LABSIM – Numerical Simulation Laboratory.

Maria Luiza Sperb Indrusiak, mlsperb@unisinos.br
Mechanical Engineering Department,Universidade do Vale do Rio dos Sinos – UNISINOS.

Nilson Romeu Marcilio, nilson@enq.ufrgs.br
Chemical Engineering Department,Universidade Federal do Rio Grande do Sul - UFRGS.

Marcelo Godinho, godinho@enq.ufrgs.br
Chemical Engineering Department,Universidade Federal do Rio Grande do Sul – UFRGS.

Abstract. The development of the design of a combustion chamber to burn leather residuals gasification gas of leather-manufacture of the region near Porto Alegre city, Rio Grande do Sul, Brazil, aims the improvement of the efficiency of the process. The thermal energy produced can be used at thermal processes within the industrial plant as well as to the electric energy production thus avoiding the consumption of conventional fuel sources. Addictionally the storage of these residuals is very expensive as they are environmentally harmful, thus needing special storage care to avoid environment contamination. However, the direct burning of this leather-residuals-gas in the chamber is not a straightforward process. The alternative developed consists in to use this residual of leather for an intermediate process of gasification or of pyrolysis and to separate the volatiles, products of partial combustion, for after use as fuel in a boiler. The boiler may be part of a Rankine power generation cycle, or also a cogeneration cycle to produce the water vapor and the hot water to the manufacture process of leather, and the electricity to the manufactory plant. Another problem related to the burning of gas-product of leather-gasification consists in the presence of environment-harmful-gases, remainings of the chemical treatment employed at leather manufacture, as cyanide, hydrocarbons as toluene, chrome and other toxic gases, as the carbon monoxide and NO_x, that must be either fully consumed in combustion process or have their production minimized, with the purpose of reduce the emission of pollutants into the atmosphere. At this way, aiming a better understanding of the combustion process and in order to obtain an improved design of this kind of furnace, an analysis of the reactive flow in the chamber was done. Different geometries and dimensions were evaluated for new designs of combustion chambers, aiming the improvement of the thermal changes, the chemical reactions rates at the process and also of the flow field. Here, it was used the commercial CFD (Computational Fluid Dynamics) software CFX © Ansys Inc. This kind of tool allows good results at low costs and time. Beyond that, with the improvement of computational technology, is possible to predict large quantity of details, obtaining solutions closer to the actual operation conditions, helping significantly the analysis of new designs of devices and equipments.

Keywords: Leather, CFD, Combustion, Finite Volumes, Waste to Energy.

1. INTRODUCTION

Among the biggest technological challenges of the present times one may cite the development of feasible technologies in order to make profitable the use of nonconventional energy sources in replacement of fossil fuels. The main reasons for that are the global warming associated with fossil fuels combustion emissions and the finite reserves of those fuels.

Another big problem that mankind must learn how to cope with is the final destination of waste. The usual disposal in landfills is no more acceptable due to harmful consequences as underground water contamination and methane emissions due to the decomposition process of the organic raw material. The allocation of large ground areas for waste disposal is also an emerging problem. As a consequence, several techniques are being studied, e.g. the collection and use of methane in energy production plants, composting, anaerobic digestion, and combustion or gasification of the waste. They are called waste to energy (WtE) technologies and present large possibilities for improvements.

Leather industry waste presents a good potential for application of such WtE technologies. There is a large quantity of industries producing leather clothes, handbags and shoes at Brazilian southeast region and discarding the residues in landfills or trenches which must be constantly monitored. Also, the creation of new waste disposal areas is not straightforward, due to restrictive environmental requirements. The legal responsibilities over the areas must also be taken into account.

Another favorable result of the combustion of leather is the ash byproduct. They are rich in chromium and can be used as raw material in the steel industry for the production of Fe-Cr alloys. They can be also recycled into chromium sulphate which is used in the tanning process. The chromium acid, used in electroplating, is another possible application. (Godinho, 2006).

The knowledge of the processes involved in the combustion and in the gasification of the biomass and in the combustion of the gases, as well as the state of the art of devices, equipments and techniques are far from being completely developed and there is space for many studies and improvements.

The efficient operation of combustion chambers of gasifiers and boilers is strongly dependent upon the oxidation reactions and heat, mass and momentum transfers occurring inside the devices. Therefore, improvements to the project of those devices are welcome. A substantial quantity of works about biomass combustion can be found in the literature, albeit few of them are related to leather combustion or gasification.

Bahillo et al. (2004) performed experimental studies on fluidized bed combustion of leather scraps. The HCN and NH_3 concentrations were measured in the reactor core and at the flue gas. According to the results, the concentrations are very low at flue gases; nevertheless they are high at the reactor core. The HCN concentration is considerably higher than that of NH_3.

Godinho et al. (2006) presented an experimental analysis of a semi-pilot plant for the processing of footwear leather wastes. The objective of the work was to evaluate the performance of the plant. The unit comprises a stratified downdraft gasifier, an oxidation reactor and an air pollution control system (APC). The results obtained in this work led to conclude that the operational conditions applied in the process provided a low degree of oxidation of the chromium content in the waste. There is also a significant participation of water-soluble compounds in the particulate matter. The low concentration of CO in the flue gas indicates high combustion efficiency for the process. A significant reduction of the NO emissions was obtained, compared to the results of the combustion of footwear leather waste in fluidized bed. The main conclusion is that the footwear leather waste (biomass) represents an alternate source for the production of electric energy. In another work, Shin et al. (2008) presents an investigation about the combustion characteristics of gas fuel in a pyrolysis-melting incinerator. The study aims to develop a novel incineration process considering the intrinsic characteristics of waste generated in Korea. The effects of secondary and tertiary air on flow pattern, mixing, and NO_x emissions of the combustion chamber were investigated. The pyrolyzed gas was simulated by propane, a mid-sized molecule among all the components. The propane was injected in the combustion chamber, and burnt through multi-step combustion by distributing the combustion air to primary, secondary, and tertiary air nozzles. Temperature and gas components in the combustion performances were determined by temperature distribution and O_2, CO and NO_x chemical species concentration. These results conclude that using the secondary and/or tertiary air, the combustion performance was improved, and, in particular, NO_x concentration decreased significantly following the tertiary air injection.

Salvador et al. (2006) presented a numerical 2D model to simulate the coupled equations for flow, heat transfer, mass transfer and progress of chemical reactions of a thermal recuperative incinerator (TRI) used to oxidize volatile organic compounds (VOCs) diluted in an air flow. The commercial software Fluent (Fluent Inc., 1998) was used. This model was confronted with experimental values obtained on a highly instrumented semi-industrial-scale pilot unit running under the same conditions. The results show that the model developed is a good tool for the analysis of combustion processes and it can predict important information about the flow, heat transfer and pollutant formation.

The work of Choi and Yi (2000) presented a numerical study of a combustion process of VOCs in a regenerative thermal oxidizer (RTO). Steady and unsteady flow field, distributions of temperature, pressure and compositions of the flue gas in the RTO were simulated by computational fluid dynamics (CFD) using the commercial software Fluent (Fluent Inc., 1998). The model system was the oxidation of benzene, toluene and xylene by the RTO, which was constituted by three beds packed with ceramic beads to exchange heat. The results show that a level of 1.0% of VOCs is sufficient to provide energy for the oxidation when heat is exchanged through the ceramic bed. A ceramic bed of 0.2 m in height is sufficient to operate properly at these conditions and 5 s is recommended as the stream switching time. In addition, the results can provide insight and practical responses involved in the design of an industrial RTO unit.
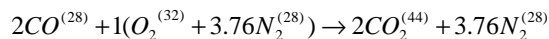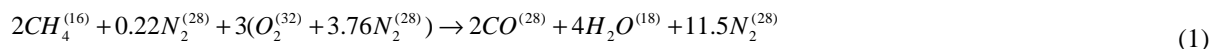
The present research work presents a numerical simulation study, using a commercial CFD code, applied to the development of an optimized design of furnace used to burn the resulting gas of the leather gasification process. The subject of the study is the analysis of combustion processes of the gas, the verification of the effect of the gas flow along the combustion chamber of a furnace of an industrial unit pilot. The main objectives are to verify the global efficiency of the burning process and to provide insight and applicable information related to the design of this kind of combustion chamber.

2. MATHEMATICAL FORMULATION

The proposed task can be stated as follows: design a combustion chamber to burn leather residual gasification gas in air, compute the temperature, chemical species concentrations and the velocity fields for gas mixture, and verify geometry features on the combustion process and pollutant formation.

Proceedings of ECOS 2009
Copyright © 2009 by ABCM

22nd International Conference on Efficiency, Cost, Optimization
Simulation and Environmental Impact of Energy Systems
August 31 – September 3, 2009, Foz do Iguaçu, Paraná, Brazil

The chemical reaction of the leather residual gasification gas used at this work, that here is considered as composed of methane, hydrogen and carbon monoxide, is modeled according to global equations presented on Westbrook and Dryer (1981), which follow:

The methane oxidation is modeled by two global steps, given by:

$$2CH_4^{(16)} + 0.22N_2^{(28)} + 3(O_2^{(32)} + 3.76N_2^{(28)}) \rightarrow 2CO^{(28)} + 4H_2O^{(18)} + 11.5N_2^{(28)}$$

$$2CO^{(28)} + 1(O_2^{(32)} + 3.76N_2^{(28)}) \rightarrow 2CO_2^{(44)} + 3.76N_2^{(28)}$$

(1)

The carbon monoxide oxidation is modeled by:

$$2CO^{(28)} + 1(O_2^{(32)} + 3.76N_2^{(28)}) \rightarrow 2CO_2^{(44)} + 3.76N_2^{(28)}$$

(2)

The hydrogen oxidation is modeled by:

$$2H_2^{(2)} + O_2^{(32)} \rightarrow 2H_2O^{(18)}$$

(3)

The formation of NO_x is modeled by Zeldovich mechanisms using two different paths, the thermal-NO and the prompt-NO, where the first, that is predominant at temperatures above 1800 K, is given by tree-step chemical reaction mechanisms:

$$O^{(16)} + N_2^{(28)} \rightarrow NO^{(30)} + N^{(14)}$$

(4)

$$N^{(14)} + O_2^{(32)} \rightarrow NO^{(30)} + O^{(16)}$$

(5)

In sub or near stoichiometric conditions, a third reaction is also used

$$OH^{(17)} + N^{(14)} \rightarrow NO^{(30)} + H^{(1)}$$

(6)

where the chemical reaction rates are predicted by Arrhenius equation.

The prompt-NO is formed at temperatures lower than 1800 K, where radicals can react rapidly with molecular nitrogen to form HCN, which may be oxidized to NO under flame conditions. The complete mechanism is not straightforward. However, De Soete proposed a single reaction rate to describe the NO source by Fennimore mechanism, which is used at this work, and the Arrhenius equations are used for predict this chemical reaction rate. At this way, the HCN oxidation to form NO is modeled by:

$$HCN^{(27)} + O_2^{(32)} \rightarrow HCO^{(29)} + NO^{(30)}$$

(7-a)

The HCN oxidation to consume the NO is

$$HCN^{(27)} + NO^{(30)} \rightarrow HCO^{(29)} + N_2^{(28)}$$

(7-b)

The HCO oxidation is modeled by

$$HCO^{(29)} + 0.75O_2^{(32)} \rightarrow CO_2^{(44)} + H_2O^{(18)}$$

(7-c)

And, to the reburning of NO by the CH$_4$ fuel gas:

$$CH_4^{(16)} + 4NO^{(30)} \rightarrow CO_2^{(44)} + 4H_2O^{(16)} + 2N_2^{(28)}$$

(7-d)

Scalar transport equations are solved for velocity, pressure, temperature and chemical species. The bulk motion of the fluid is modeled using single velocity, pressure, temperature, chemical species and turbulence fields.

2.1. Mass and species conservation

Each component has its own Reynolds-averaged equation for mass conservation, which, considering incompressible and stationary flow can be written in tensor notation as a mixture faction of all components. So, the standard continuity equation can be written as

$$\frac{\partial\left(\tilde{\rho}_i \tilde{U}_j\right)}{\partial x_j} = 0$$

(8)

where $\tilde{U}_j = \sum\left(\tilde{\rho}_i \tilde{U}_{ij}\right)\Big/\overline{\rho}$. $\tilde{\rho}_i$ and $\overline{\rho}$ are respectively the mass-average density of fluid component i in the mixture and the average density, x is the spatial coordinate, and $\tilde{U}_{ij}$ is the mass-averaged velocity of fluid component i.

The mass fraction of component i is defined as $\tilde{Y}_i = \bar{\rho}_i / \bar{\rho}$. Substituting this expressions into Eq. (8) and modeling the turbulent scalar flows using the eddy dissipation assumption it follows that

$$\frac{\partial}{\partial x_j}\left(\bar{\rho}\,\tilde{U}_j\,\tilde{Y}_i\right) = \frac{\partial}{\partial x_j}\left(\left(\rho D_i + \frac{\mu_t}{Sc_t}\right)\frac{\partial \tilde{Y}_i}{\partial x_j}\right) + S_i \tag{9}$$

where D_i is the kinematic diffusivity, μ_t is the turbulent viscosity and Sc_t is the turbulent Schmidt number. Note that the sum of component mass fractions over all components is equal to one.

2.2. Momentum conservation

For the fluid flow the momentum conservation equations are given by:

$$\frac{\partial}{\partial x_j}\left(\bar{\rho}\,\tilde{U}_i\,\tilde{U}_j\right) = -\frac{\partial p^*}{\partial x_j}\delta + \frac{\partial}{\partial x_j}\left(\mu_{eff}\frac{\partial \tilde{U}_i}{\partial x_j}\right) + \frac{\partial \tilde{U}}{\partial x_j \partial x_i} + S_U \tag{10}$$

where $\mu_{eff} = \mu + \mu_t$ and μ is the mixture dynamic viscosity and μ_t is the turbulent viscosity, defined as $\mu_t = C_\mu \rho\, k^2 / \varepsilon$. The term $p^* = \bar{p} - (2/3)k$ is the modified pressure, C_μ is an empirical constant of the turbulence model, $\bar{p}$ is the time-averaged pressure of the gaseous mixture, and δ is the Krönecker delta function. S_U is the source term, introduced to model the buoyancy and drag force due to the transportation particles, and other mathematical terms due to turbulence models. The Boussinesq model is used to represent the buoyancy force due to density variations.

2.3. The $k - \varpi$ turbulence model

The equations for turbulent kinetic energy, k, and its turbulent frequency, ϖ, are:

$$\frac{\partial}{\partial x_j}\left(\tilde{\rho}\,\tilde{U}_j\,k\right) = \left(\frac{\partial}{\partial x_j}\left(\mu + \frac{\mu_t}{\sigma_k}\right)\frac{\partial k}{\partial x_j}\right) + \left[\mu_t\left(\frac{\partial U_i}{\partial x_j} + \frac{\partial U_j}{\partial x_i}\right)\right] - \beta'\rho k\varpi \tag{11}$$

$$\frac{\partial}{\partial x_j}\left(\tilde{\rho}\,\tilde{U}_j\,\varpi\right) = \left(\frac{\partial}{\partial x_j}\left(\mu + \frac{\mu_t}{\sigma_\varpi}\right)\frac{\partial \varpi}{\partial x_j}\right) + \alpha\frac{\varpi}{k}\left[\mu_t\left(\frac{\partial U_i}{\partial x_j} + \frac{\partial U_j}{\partial x_i}\right)\right] - \beta\rho\varpi^2 \tag{12}$$

where β', β and α are empirical constants of the turbulence model, σ_k and σ_ϖ are the Prandtl numbers of the kinetic energy and frequency, respectively.

2.4. Energy conservation

Considering the transport of energy due to the diffusion of each chemical species, the energy equation can be written as

$$\frac{\partial}{\partial x_j}\left(\bar{\rho}\,\tilde{U}_j\,\tilde{h}\right) = \frac{\partial}{\partial x_j}\left(\left(\mu + \frac{\mu_t}{\mathrm{Pr}_t}\right)\frac{\partial \tilde{h}}{\partial x_j} + \sum_i^{Nc}\bar{\rho}D_i\,\tilde{h}_i\frac{\partial \tilde{Y}_i}{\partial x_j} + \frac{\mu_t}{\mathrm{Pr}_t}\frac{\partial \tilde{h}}{\partial x_j}\right) + S_{rad} + S_{rea} \tag{13}$$

where $\tilde{h}$ and c_p are the average enthalpy and specific heat of the mixture. The latter is given by $c_p = \sum_\alpha \tilde{Y}_\alpha c_{p,\alpha}$, where $c_{p,\alpha}$ and $\tilde{Y}$ are the specific heat and the average mass fraction of the α-th chemical species, κ is the thermal conductivity of the mixture, Pr_t is the turbulent Prandtl number, and S_{rad} and S_{rea} represent the sources of thermal energy due to the radiative transfer and to the chemical reactions. The term S_{rea} can be written as:

$$S_{rea} = \sum_\alpha \left[\frac{h_\alpha^0}{MM_\alpha} + \int_{\tilde{T}_{ref,\alpha}}^{\tilde{T}} c_{p,\alpha}\,d\tilde{T}\right]R_\alpha \tag{14}$$

where $\tilde{T}$ is the average temperature of the mixture, h_α^0 and $\tilde{T}_{ref,\alpha}$ are the formation enthalpy and the reference temperature of the α-th chemical species. To complete the model, the density of mixture can be obtained from the ideal

Proceedings of ECOS 2009
Copyright © 2009 by ABCM

22nd International Conference on Efficiency, Cost, Optimization
Simulation and Environmental Impact of Energy Systems
August 31 – September 3, 2009, Foz do Iguaçu, Paraná, Brazil

gas equation of state (Kuo, 1996; CFX Inc., 2004; Turns, 2000), $\overline{\rho} = p\overline{MM}\left(\overline{R}\tilde{T}\right)^{-1}$, where p is the combustion chamber operational pressure, which is here set equal to 1 atm (Spalding, 1979), and $\overline{MM}$ is the mixture molecular mass. The aforementioned equations are valid only in the turbulent core, where $\mu_t >> \mu$. Close to the wall, the logarithmic law of the wall is used (Launder and Sharma, 1974).

To consider thermal radiation exchanges inside the combustion chamber, the Discrete Transfer Radiation Model - DTRM is employed (Carvalho et al., 1991), considering that the scattering is isotropic. The effect of the wavelength dependence is not considered, and the gas absorption coefficient is considered uniform inside the combustion chamber and its value is 0.5 m^{-1}. Then, the Radiative Transfer Equation – RTE is integrated within its spectral band and a modified RTE can be written as

$$\frac{dI(r,s)}{dS} = \frac{K_a \sigma \tilde{T}^4}{\pi} - K_a I(r,s) + S^{"} \tag{15}$$

At the equations above, σ is the Stefan-Boltzmann constant (5.672 x 10^{-8} W/m^{2}K^4), r is the vector position, s is the vector direction, S is the path length, K_a is the absorption coefficient, I is the total radiation intensity which depends on position and direction, and $S"$ is the radiation source term, which can incorporate the radiation emission of the particles, for example.

2.5. The E-A (Eddy Breakup – Arrhenius) chemical reactions model

The reduced chemical reactions model that is employed here assumes finite rate reactions and a steady state turbulent process to volatiles combustion. In addition, it is considered that the combined pre-mixed and non-premixed oxidation occurs in two global chemical reaction steps, and involves the follow species: oxygen, methane, hydrogen, nitrogen, water vapor, carbon dioxide and carbon monoxide. A conservation equation is required for each species, with the exception of nitrogen. Thus, one has the conservation equation for the α-th chemical species, given by Eq. (9), where the source term, S_i, considers the average volumetric rate of formation or destruction of the α-th chemical species at all chemical reactions. This term is computed from the summation of the volumetric rates of formation or destruction in all the k-th equations where the α-th species is present, $\overline{R_{\alpha,k}}$. Thus, $\overline{R_\alpha} = \sum_k \overline{R_{\alpha,k}}$.

The rate of formation or destruction, $\overline{R_{\alpha,k}}$, can be obtained from an Arrhenius kinetic rate relation, which takes into account the turbulence effect, such as Magnussen equations (Eddy Breakup) (Magnussen and Hjertager, 1976), or a combination of the two formulations, the so called Arrhenius-Magnussen model (Eaton et al., 1999; CFX Inc., 2004). Such relations are appropriate for a wide range of applications, for instance, laminar or turbulent chemical reactions with or without pre-mixing. The Arrhenius equation can be written as follows:

$$\overline{R_{\alpha,k,Chemical}} = -\eta_{\alpha,k}\overline{MM}_\alpha \tilde{T}^{\beta_k} A_k \Pi_\alpha \tilde{C}_\alpha^{\gamma_{\alpha,k}} \exp\left(\frac{-E_k}{\overline{R}\tilde{T}}\right) \tag{16}$$

where β_k is the temperature exponent in each chemical reaction k, which is obtained empirically together with the energy activation E_k and the coefficient A_k. Π_α is the product symbol, $\tilde{C}_\alpha$ is the molar concentration of the α-th chemical species, $\gamma_{\alpha,k}$ is the concentration exponent in each reaction k, $\overline{R}$ is the gas constant, $\overline{MM}_\alpha$ and $\eta_{\alpha,k}$ are the molecular mass and the stoichiometric coefficient of α in the k-th chemical reaction.

In the Eddy-Breakup or Magnussen model, the chemical reaction rates are based on the theories of vortex dissipation in the presence of turbulence. Thus, for diffusive flames:

$$\overline{R_{\alpha,k,EBU}} = -\eta_{\alpha,k}\overline{MM}_\alpha A \overline{\rho} \frac{\varepsilon}{k} \frac{\tilde{Y}_{\alpha^*}}{\eta_{\alpha^*,k}\overline{MM}_{\alpha^*}} \tag{17}$$

where the index α^* represents the reactant α that has the least value of $\overline{R_{\alpha,k,EBU}}$.

In the presence of premixing, a third relation for the Eddy Breakup model is necessary, so that

$$\overline{R_{\alpha,k,Premixing}} = \eta_{\alpha,k}\overline{MM}_\alpha AB\overline{\rho} \frac{\varepsilon}{k} \frac{\sum_p \tilde{Y}_p}{\sum_p \eta_{p,k}\overline{MM}_p} \tag{18}$$

where the index p represents the gaseous products of the combustion. A and B are empirical constants that are set as 4 and 0.5 (Magnussen and Hjertager, 1976). Magnussen model, Eqs. (17) and (18), can be applied to both diffusive and pre-mixed flames, or for the situation where both flames coexist, taking the smallest rate of chemical reaction.

Finally, for the Arrhenius-Magnussen model, given by Eqs. (16), (17) and (18), the rate of formation or destruction of the chemical species is taken as the least one between the values obtained from each model. It follows that

$$\overline{R_{\alpha,k}} = \min\left(\overline{R_{\alpha,k,Chemical}}, \overline{R_{\alpha,k,EBU}}, \overline{R_{\alpha,k,Premixed}}\right) \tag{19}$$

3. FURNACE DESCRIPTION

The furnace is a model already used for experimental studies and comprises four tubular segments. The segments are made of refractory concrete. The first two and the fourth segments have a coaxial external tube (jacket) that creates an annular region where air is preheated. The combustion chamber comprises the first segment of the furnace, where a mixture of primary air and fuel is injected. The secondary air is forced by a blower from the inlet at the upper region of the second segment through the annular tube and is injected into the combustion chamber by means of several small holes evenly distributed along the first segment. The auxiliary air that enters at the lower part of the fourth segment is preheated at the annular region, than premixed with fuel oil and injected through the two auxiliary burners (Fig 1) during the startup of the plant. After the startup period, the auxiliary burners act as tertiary air feeders.
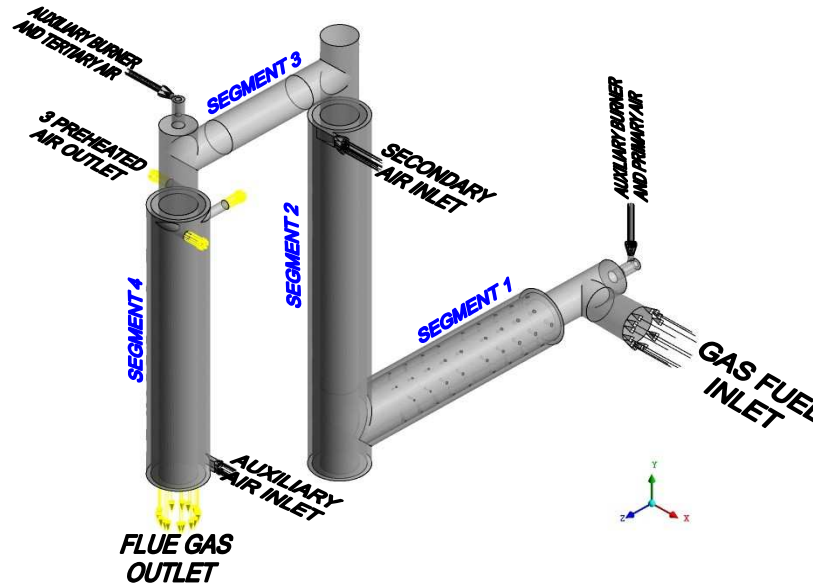

Figure 1 - General disposition of the furnace.

4. MESH SETTINGS AND CONVERGENCE CRITERIA

The domain under consideration comprises the furnace of a gasification/combustion plant to convert biomass in energy: the furnace comprises a tubular riser where occurs the combustion process of residual gasification gas as showed at Fig. 1. The entrance to furnace was considered the outlet of the domain. The discretization was done using tetrahedrical volumes. Prismatic volumes were used at the walls in order to capture the boundary layer behavior. Due to computational limitations, the mesh size used has approximately 2.8×10^6 elements, using mesh refinements in the entrance region, corresponding to the first part of furnace. The convergence criterion adopted was the RMS – Root Mean Square of the residual values, and the value adopted was 1×10^{-6} for all equations.

5. BOUNDARY CONDITIONS

In order to simulate the leather residual gasification gas, a fuel compounded of H_2O, N_2, CO, HCN, CO_2, H_2 and CH_4 was used. The species concentrations attributed to the fuel are shown in Tab. 1. It was considered that the mass flow of this gas is 740 kg/h at inlet uniform temperature of 800 ºC. This temperature value was set considering the heating on gasification process.

The composition of the air for the combustion process was the usual one (23% of O_2 and 77% of N_2). The temperature of inlet secondary air is 25 ºC, the same temperature of ambient air around the plant, and its mass flow is 720 kg/h. The inlet air in the auxiliary burners (primary and tertiary air) is heated in the pre-heater at segment 4, and its mass flow is 90 kg/h for each burner. Also, it was considered that the insulation used at the furnace wall has a thermal conductivity of approximately 1.4 W/(m·K) and its density is 2300 kg/m^3. It was not considered at this simulation the thermal resistance of the metallic walls.

Proceedings of ECOS 2009
Copyright © 2009 by ABCM

22nd International Conference on Efficiency, Cost, Optimization
Simulation and Environmental Impact of Energy Systems
August 31 – September 3, 2009, Foz do Iguaçu, Paraná, Brazil

Table 1 – Chemical composition of inlet fuel gas.

	Mass fraction	Mass flow [kg/h]		Mass fraction	Mass flow [kg/h]
H_2O	0.076	56.24	CO_2	0.230	170.20
O_2	-	-	H_2	0.007	5.18
N_2	0.642	475.08	CH_4	0.012	8.88
CO	0.032	23.68	HCN	0.001	0.74

6. RESULTS

The initial project of the furnace presented several problems like incomplete combustion and flame blow-out. The last one may cause a severe failure of the plant. The cause of the problem was identified as being the improper position and temperature of the air injection. The air was injected at room temperature along a large extension of the first segment of the installation, where is located the combustion chamber. In addition the resultant low temperature of the mixture determined the partial combustion of the fuel and consequently the presence of a large amount of pollutants in the flue gases. In order to solve the problem some new designs were proposed, concerning the furnace geometry and also the secondary air injection system, primary air and fuel mixture and auxiliary burners disposition.

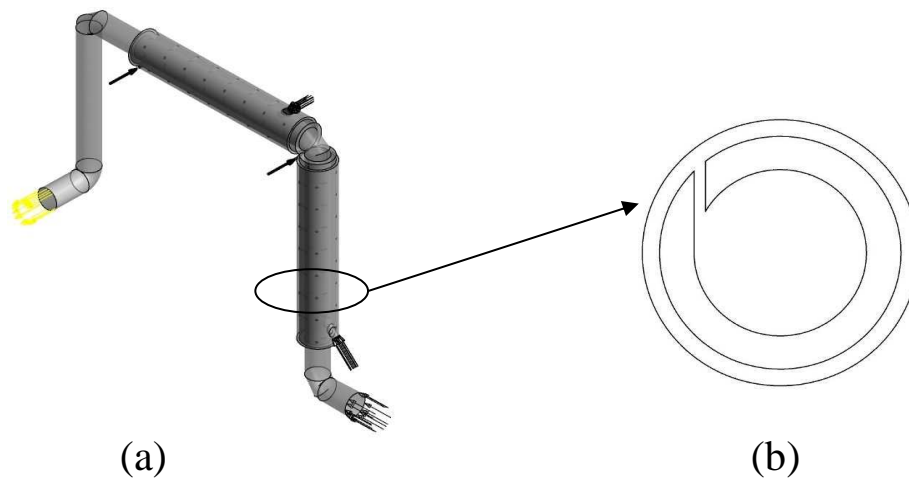(a)   (b)

Figure 2 – Start-up project of furnace: (a) isometric view; (b) transversal cross section under pre-heater.

The first new design (Fig. 3) removed the jacket of the second section in order to modify the heat transfer characteristics of secondary air. The secondary air inlet was moved to the top of jacket to create a counter-flow to enhance the heat transfer of this air. The holes for the distribution of the secondary air were evenly distributed along 2/3 of the segment length. The remaining part acts as a preheater of the air (Fig. 3-a). The modification improved the efficiency of the combustion. Nevertheless, as shown at Fig. 3, the simulation shows that the temperatures are still too low and the air is not being properly preheated. Additionally, the flame profile is not homogeneous at the combustion chamber thus allowing the contact with the walls and damaging them. The heterogeneous mixture of air and fuel, due to the curve at the inlet gives rise to the problem.

Secondary air
pre-heater

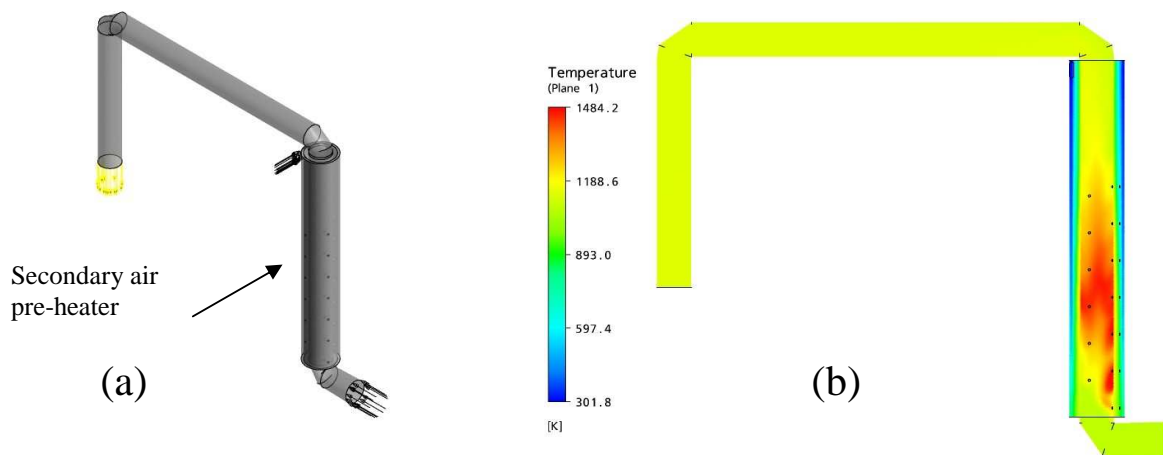(a)   (b)

Figure 3 – First modification of furnace: (a) isometric view; (b) temperature field in longitudinal cross section.

The second improvement proposed is related to the quantity and spatial distribution of the secondary air injection holes. They are now positioned along the first 1/3 of the segment length, allowing the remaining 2/3 for the preheating of the air (Fig. 4). The change improves significantly the secondary air temperature albeit the increase was still not enough. Also, due to the reduction in the number of the holes, the velocity of the air entering the combustion chamber is increased, promoting a strong perturbation in the main stream of gases, disturbing the development of the combustion process.

Figure 5-a shows by means of streamlines the detail of the primary and secondary air in a transverse section of the combustion chamber (first segment). The velocity field in a longitudinal plane of the combustion chamber is shown at Fig. 5-b. The velocity values at the holes are presented in order to emphasize their distribution
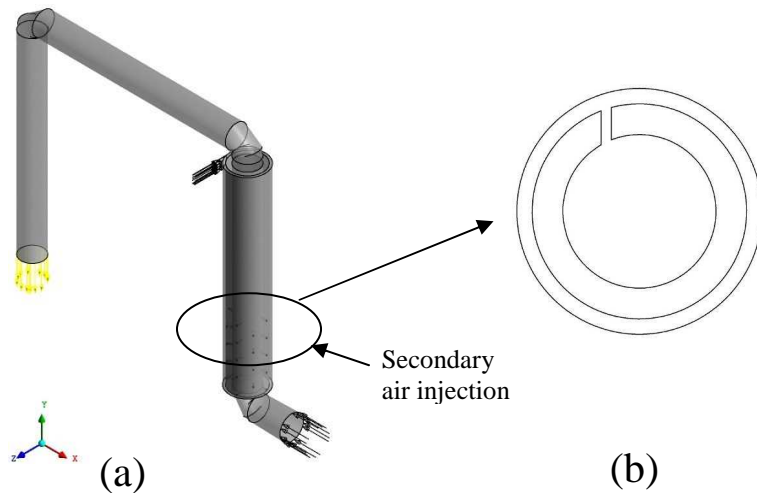

(a)   (b)

Figure 4 – Second modification of furnace: (a) isometric view; (b) transversal cross section under pre-heater.

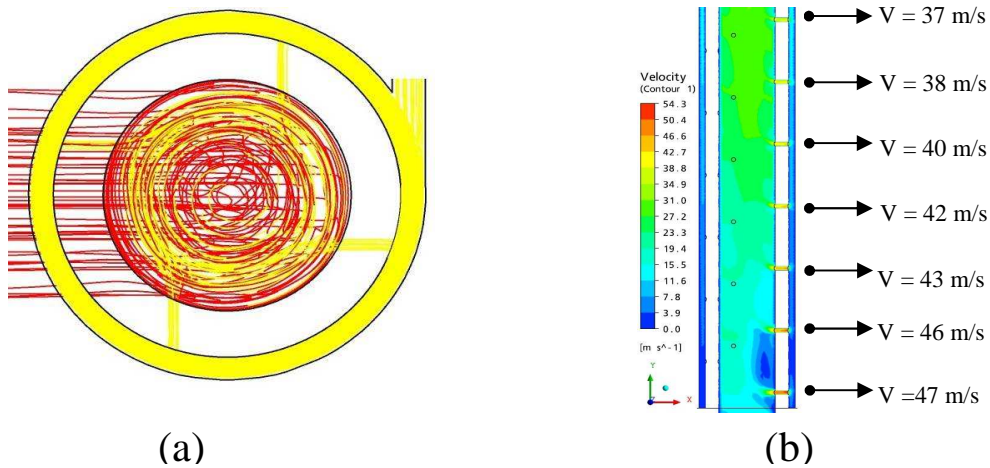(a)   (b)

Figure 5 – Cross section view of furnace combustion chamber: (a) streamlines; (b) velocity field.

The third modification was an extension of the preheating chamber with the inclusion of the second segment, properly jacketed. The holes in the first segment were made along the whole segment thus allowing a better air injection distribution and also lower velocities. The spatial disposition of the furnace was also modified, in order to achieve a better utilization of the available space.

The simulation showed that this last design presented the best combustion efficiency. The temperatures of the secondary air were on the order of 500 ^{o}C at the combustion chamber outlet region and 700 ^{o}C at the inlet region, inducing a homogeneous flame profile. Figure 6-a shows the temperature field at a longitudinal plane. The flame core temperatures are of the order of 1700 ^{o}C, resulting in a more efficient combustion and less pollutants in flue gases. Figure 6-b shows the hydrogen concentration at the same longitudinal plane.

Figures 7-a and 7-b show the resulting concentration field for CO and CH$_4$. The results of Fig. 6-b, 7-a and 7-b allow the conclusion that all the combustible is oxidized in the first half part of the combustion chamber (segment 1) and the resulting flame occupies all the combustion chamber segment.

Proceedings of ECOS 2009
Copyright © 2009 by ABCM

22nd International Conference on Efficiency, Cost, Optimization
Simulation and Environmental Impact of Energy Systems
August 31 – September 3, 2009, Foz do Iguaçu, Paraná, Brazil
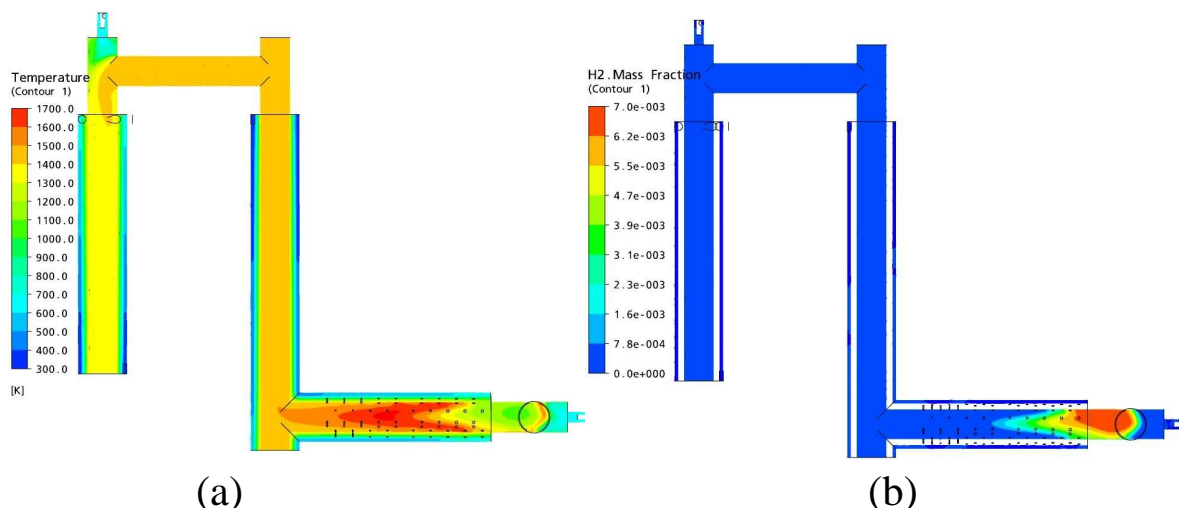
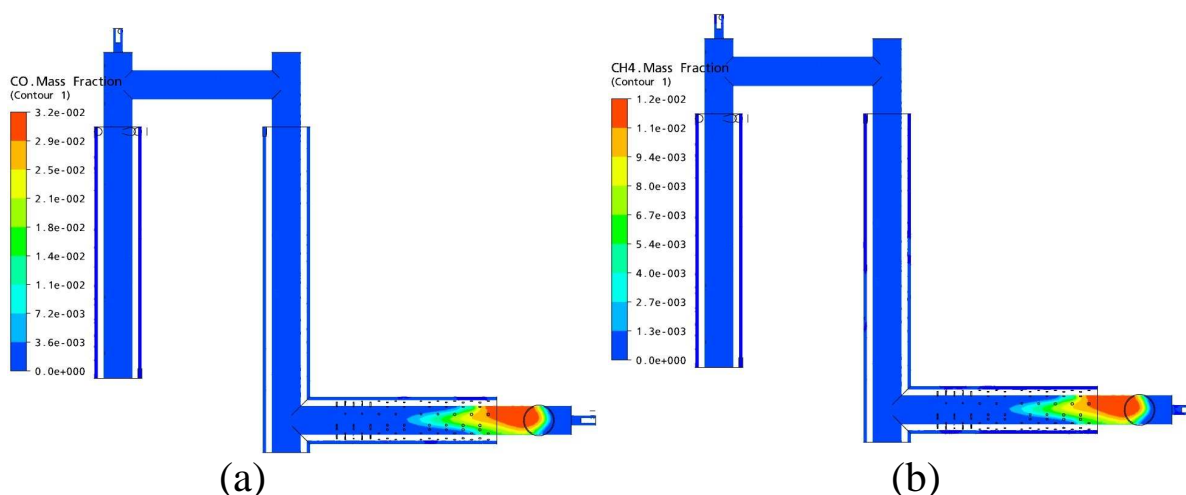Figure 6 – (a) Temperature field; (b) Hydrogen concentration.

Figure 7 – (a) Carbon monoxide concentration; (b) Methane concentration.

The concentration field of HCN and NO_x (thermal + prompt + fuel) were presented at Fig. 8-a and 8-b. The higher carbon dioxide concentrations are also at segment 1, as expected. In the next segments the combustion products are diluted with the secondary and tertiary air. Fig 8-b shows also that there is a high rate of NO_x formation along the furnace, especially at combustion chamber down flow, where the temperature is the higher one. Indeed, Fig. 6-a shows temperatures on the order of 1300 to 1500 K, high enough to enhance the production of NO_x by the Fennimore mechanism. Besides, one can observe that HCN and NO_x concentrations have an inverse relation; the concentration of one reduces where the concentration of other enhances. The high level of excess air and the large residence time of the flue gases in the furnace also contribute somewhat to the NO_x production.

The last modification consisted of the reallocation of the two startup burners, which use kerosene as fuel and after the initial period are responsible by the tertiary air. In order to pre heat the tertiary air a jacket was added to the fourth segment of the furnace, similarly to that was already done at the other segments. The preheated air was used at the auxiliary burners and also at the first process (gasification) not shown in this work. Figure 1 shows the furnace with all the described modifications.

7. CONCLUSIONS

The proposed modifications (Fig. 1) have as result an improved design with better performance them the initial project (Fig. 2). The new secondary air injection design (segments 1 and 2) along with the relocation of the auxiliary burners have a special role in the improved performance due to the better mixing of the main and secondary flows, thus allowing a better air distribution in the chamber.

Contrasting the temperature fields for initial and final design (Fig. 3-b and 6-a respectively) one can see that the alteration introduced in the secondary air pre-heater improves substantially the efficiency of the gas burning process, with higher gas temperatures inside the chamber. The higher temperatures along the furnace allowed the installation of the air preheater at the segment 4, in order to preheat the primary and tertiary air, leading to another improvement of the

combustion process. Additionally this second preheater generates a supplementary quantity of air to the gasification process, thus enhancing the global efficiency of the plant. Another important conclusion is that the obedience to CONAMA, the Brazilian Counsel of Environment, determinations for CO limits, which determines a high value of excess air, enhances significantly the NO_x production.
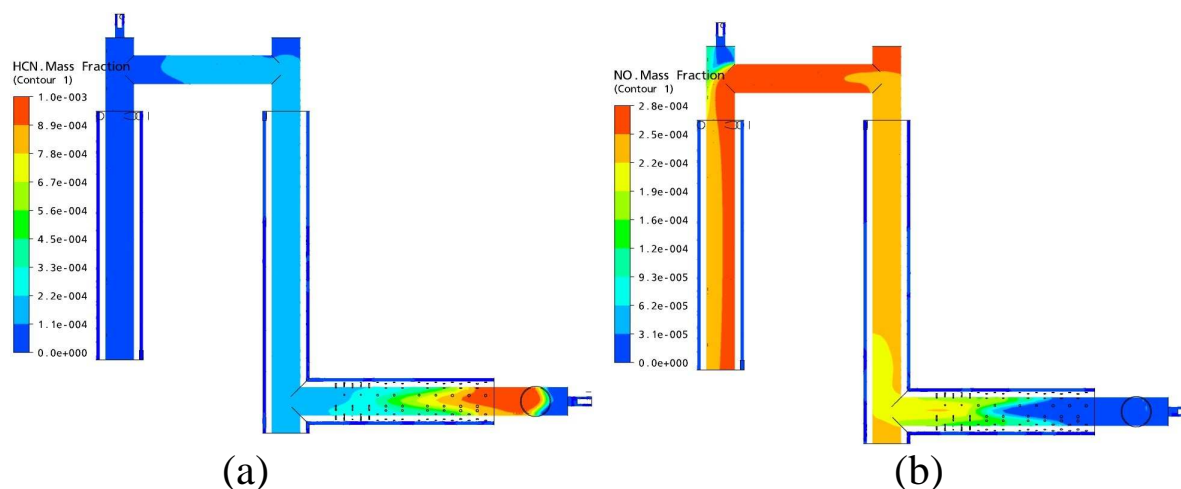

(a)   (b)

Figure 8 – (a) HCN concentration; (b) NOx concentration.

8. REFERENCES

Bahillo, A., Armesto, L., Cabanillas, A. and Otero, J., 2004. "Thermal valorization of footwear leather wastes in bubbling fluidized bed combustion". Waste Management, Vol. 24, pp. 935-944.

Carvalho, M.G., Farias, T. and Fontes, P., 1991. "Predicting radiative heat transfer in absorbing, emitting, and scattering media using the discrete transfer method", ASME HTD, Vol. 160, pp.17-26.

CFX Solver Theory, 2004.

Choi, B.S. and Yi, J., 2000. "Simulation and optimization on the regenerative thermal oxidation of volatile organic compounds". Chemical Engineering Journal, Vol. 73, pp. 103-114.

CONAMA – Conselho Nacional do Meio Ambiente, Ministério do Meio Ambiente, Resolução n° 316, de 29 de outubro do 2002. <<http://www.mma.gov.br/port/conama/legiabre.cfm?codlegi=338>>

Eaton, A. M., Smoot, L. D., Hill, S. C. and Eatough, C. N., 1999, "Components, formulations, solutions, evaluations, and applications of comprehensive combustion models", V. 25, pp. 387-436.

Fluent User's Guide, vol. 2, 1998.

Godinho, M., 2006 "Gaseificação e combustão de resíduos sólidos da indústria calçadista". Doctoral Thesis, Programa de Pós-Graduação em Engenharia de Minas, Metalúrgica e de Materiais (PPGEM), Universidade Federal do Rio Grande do Sul, Brazil.

Godinho, M., Marcilio, N.R., Faria Vilela, A.C., Masotti, L. and Martins, C.B. 2007 "Gaseification and combustion of the footwear leather wastes". Jalca, Vol. 102, pp. 182-190

Kuo, K.K., 1996. "Principles of combustion", John Wiley & Sons, New York.

Launder, B.E. and Sharma, B.I., 1974. "Application of the energy-dissipation model of turbulence to the calculation of flow near a spinning disc", Letters in Heat and Mass Transfer, Vol. 19, pp. 519-524.

Magnussen B.F. and Hjertager B. H., 1976. "On mathematical models of turbulent combustion with special emphasis on soot formation and combustion". Proc. of the 16th Int. Symp. on Comb., The Combustion Institute, pp. 719–729.

Salvador, S., Commander, J.M. and Kara, Y., 2006. "Thermal recuperative incineration of VOCs: CFD modeling and experimental validation". Applied Thermal engineering, Vol. 26, pp. 2355-2366.

Shin, D., Yu, T., Yang, W., Jeon, B., Park, S. and Hwang, J., 2008. "Combustion characteristic of simulated gas fuel in a 30 kg/h scale pyrolysis-melting incinerator". Waste Management, IN PRESS.

Spalding, D.B., 1979. "Combustion and Mass Transfer", Pergamon Press, Inc., New York.

Westbrook, C. K. and Dryer, F.L., 1981. "Simplified reaction mechanisms for the oxidation hydrocarbon fuels in flames". Comb. Sci. and Technology, Vol. 27, pp. 31-43.

Turns, S. T., 2000, "An introduction to combustion – Concepts and applications", 2nd ed, McGraw-Hill, New York.

RESPONSIBILITY NOTICE

The authors are the only responsible for the printed material included in this paper.